Fabrication of Different Morphologies Micro-/nano- Dual-scale Super-hydrophobic Al_2O_3 Surface

Wei Hu [1, 2, *], Dafeng Yang [1, 2], Guoquan Liu [1, 2], Changbing Chen [1, 2]

[1] Research Institute for National Defense Engineering of Academy of Military Science, PLA, Luoyang 471023, China

[2] Henan Key Laboratory of Special Protective Materials, Luoyang 471023, China

* Corresponding author e-mail: huwei@nuaa.edu.cn

Abstract. The preparation of super-hydrophobic surface by alumina usually uses indirect assembly methods, such as template method, deposition method, sol-gel method, etc., and super-hydrophobic Al_2O_3 surface with different micro-/nano- dual-scale structure is rarely obtained by direct oxidation method. In this study, lotus leaf-like super-hydrophobic surface alumina films with different micro-/nano- dual-scale structures were prepared by third-step anodic oxidation, no other assembly steps are required. The changes of surface morphology, hydrophobic property of Al_2O_3 films under different length of time of third-step anodization were analyzed, the results prove that the super-hydrophobic Al_2O_3 films have large contact angle CA (CAmax=158.6°).

Keywords: Al_2O_3 Surface; Large Contact Angle CA; Super-hydrophobic.

1. Introduction

The 'Lotus effect' of the lotus leaf has attractive 'self-cleaning' property, therefore, a great deal of studies have been carried out by mimicking the lotus leaf in various ways to demonstrate an artificial super-hydrophobic surface with the CA >150° [1, 2]. The hydrophobicity of such surfaces can be obtained from the increase in surface roughness, especially, it has been fabricated the micro-/nano-dual-scale roughness can improve a surface's super-hydrophobicity to a considerable extent compared to surfaces with nano- mono-roughness. Most commonly, vertical-walls micro-pillar structures modified with micro-/nano- dual-scale roughness have been used to construct bionic hydrophobic surface materials [3-6]. A series of surface geometries including grooves, encompassing pillars, holes and honeycombs have been studied, however, the wettability of such structures is usually depending on their feature sizes and arrangement. For example, a honeycomb structure can maintain super-hydrophobicity under elevated water pressure, which translates into resistance to droplets impingement [7-10]. This capability is important because a transition from the fully wetting Wenzel state to a nonwetting Cassie model [11].

Ceramic structure Al_2O_3 has a shape like beehive, it has porous surface morphology. In this study, Al_2O_3 films with the unfair hole porous ceramic structure surface and rough super-hydrophobic surface full of many nanobulges were prepared by third-step anodic oxidation at low current density (18 mA/cm^2) in mixed phosphoric acid and oxalic acid solution under low temperature conditions. Their changes in surface roughness and corrosion resistance were evaluated according to the physicochemical properties of the obtained Al_2O_3 films, the results show that the super-hydrophobic surfaces have good corrosion resistance, and their CA increase with the formation of micro-/nano-dual-scale roughness structure [12].

2. Experimental

2.1 Experimental Part

High purity aluminum (Al 99.99 % of the purity, thickness 200 μm) was cut into 1 cm × 2 cm thin sheets, annealed in a 500℃ tubular vacuum furnace for 3 h under nitrogen atmosphere, and then annealed in a 500 ℃ vacuum for 5 h, and afterwards the ultrasonic cleaning was performed in absolute

ethyl alcohol for 20 min to remove dirt on surface, 1 $mol \cdot l^{-1}$ NaOH was applied for 1 min to remove surface oxide. Finally, aluminium shirts were put into 1 $mol \cdot l^{-1}$ HNO_3 to neutralize OH^- 2 min, Wash and dry with distilled water. All chemicals are analytical.

Anodization was performed in the 0.4 $mol \cdot l^{-1}$ oxalic acid and 5 % by weight (wt.) phosphoric acid solution (concentration ratio 1:1) were used as electrolyte, lead plate as cathode and aluminum plate as anode for 2 h at 10°C and constant 50 V DC voltage. Then, washed the aluminum sheet with distilled water, and soak in a mixture of 6 wt.% phosphoric acid and 1.8 wt.% chromate was immersed at 60℃ for 3 hours to eliminate the irregular oxide layer produced in the oxidation process. The second anodic oxidation was carried out for 3 hours under the same conditions as the first anodic oxidation. The third anodic oxidation was carried out for 20-60 min at 5°C and constant 50 V DC voltage. The final Al_2O_3 film was washed with distilled water and dried in air oven under 45 °C for 5 min at 20 m/s airflow velocity until the surface of sample is dry.

2.2 Test Methods

JSM-6360LV electron was used to analyze the microscope scanning electronic microscopy (SEM) on the surface of alumina film to observe upper surface and transverse section of the film. The static CA of the film was measured by CA meter (0CAH 200).

3. Results and Discussion

3.1 Scanning Electronic Microscopy (SEM) Analysis

Figure 1 (a-d) shows SEM photos of samples with different time of secondary oxidation: 60 min (a), 75 min (b), 90 min (c) and 100 min (d), from the intuitive point of view, as the voltage increases, the porous layers are looser and the more obvious the stratification of the porous structure in the vertical direction. The surface of anodized alumina has a porous, uniform and multilayer loose honeycomb structure, he holes are communicated with each other, and most of the holes are in an opening state, the average diameter of which may be about 100 nm, there are faults between the hole and the hole. The overlapping porous structure looks like a honeycomb from the front view (Figure 1 a, b). As the depth of the alumina tube and the fracture surface, corrosion occurred from the lateral side, tube rupture, resulting in layered structure. Because of the different depth and fracture of the alumina tubes, a staggered honeycomb structure alumina film is formed in Figure 1 (d).

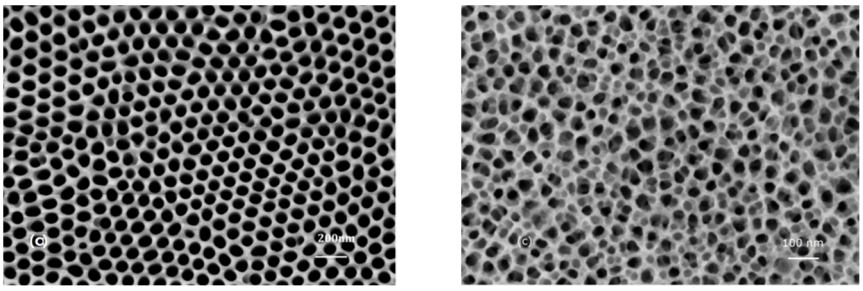

(a) and AAO film (b) from top view under magnification of 2000

Figure 1. SEM images of honeycomb-like alumina film

Figure 2 is the SEM images of the Al_2O_3 films with different time of the third-step oxidation. With the time of third-step anodization more than 30 min, the Al_2O_3 pore walls were further etched (a). A large number of needle-like protrusions were combined into clusters to form sharp island-like structure protrusions cover the porous substrate (d), when the time of third-step anodization reaches 50 min, and the small island-like protrusions were further aggregated to form ridge-like structure surface (e). Figure 2 (f) is the cross-section image of the Al_2O_3 films, shows that the alumina tubular

is may due to the effect of corrosion current or other factors to not grow deeper, but produce new short tubes in different faults and still has a micro/nano dual-scale structure (j).

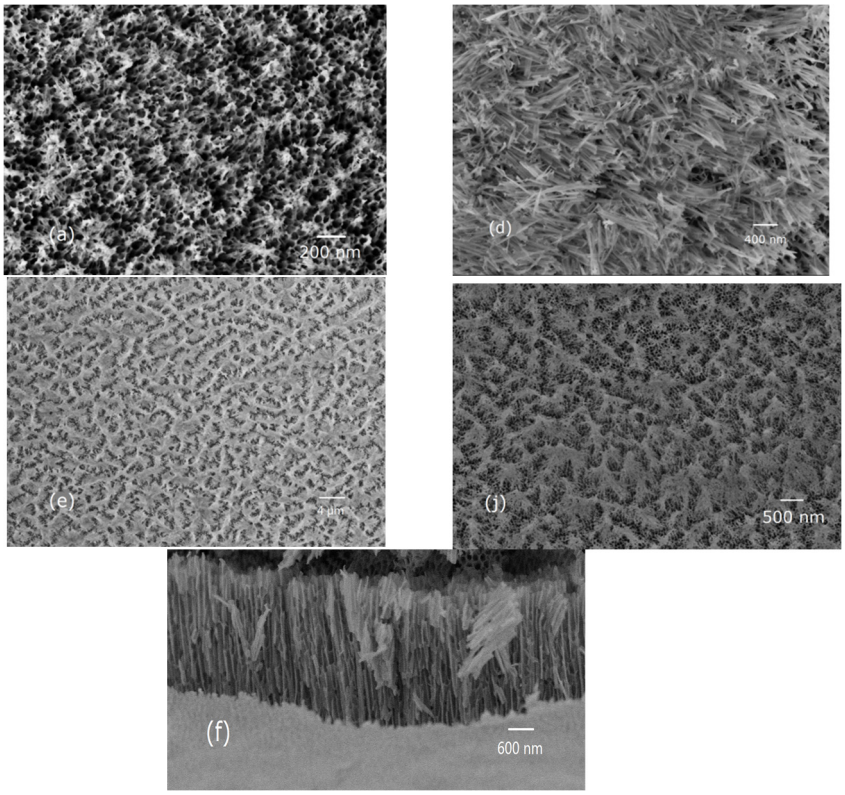

Figure 2. SEM images of oxide films with different time of the third-step oxidation

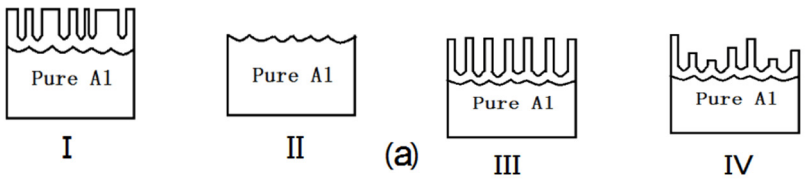

Figure 3. Growth mechanism of alumina film.

Through SEM analysis of alumina film, it can be suggested that the formation of this alumina film's ceramics structure has the following steps:

(i) The process of downward growth of alumina tube. In the second of the anodic oxidation, with the electrochemical reaction, Al undergoes pitting corrosion and forms vertical alumina tubelines at a high current density by constructing thin walls between the holes, as shown in Figure 3 (I).

(ii) The nonuniform alumina film on the surface was then removed with a mixed acid, as shown in Figure 3 (II), and the voids left on the surface of pure aluminum are favorable for the formation of regular hexagonal hole surfaces.

(iii) Holes are generated in the direction of the electric field starting from the position of pits (Figure 3 II), the volume between each of the two adjacent alumina tubes is different, and the high purity aluminum substrate and alumina membrane lead to a large stress inside the alumina film. The holes grow steadily as they conform position to each other and the alumina pores have a good selectivity orientation and become ordered (Figure 3 III). In addition, the new micropores also increase the electric resistance on the sample surface. Because of the different depth and fracture of the alumina tube, a staggered honeycomb structure alumina film is formed, as shown Figure 3 (IV). From the top view, it looks like the reinforced concrete frame, the following mechanical properties and electromagnetic properties also prove the role of this morphology.

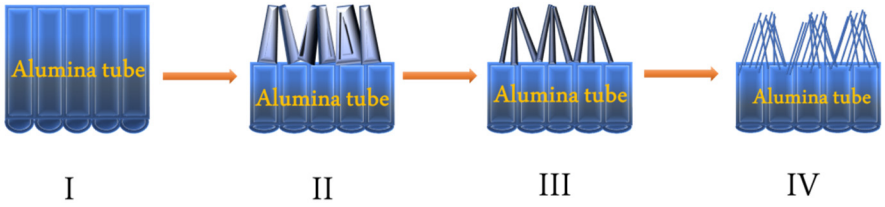

Figure 4. Surface morphologies of super-hydrophobic oxide films gradual change with the third-step oxidation time

Figure 4 is the mechanism of the evolution process from nanopores structure to the Al_2O_3 nanowires pyramids-like structure (WPOP) surface, it can be seen that three super-hydrophobic nanostructures are likely to be shapes formed by stacking the residual pore walls after etching the side walls of tubes. The Al_2O_3 forms a common hexagonal nanopore structure during the initial anodization stage (Figure 4 (I) and Figure 1 (b)). Then the anodization reaction evolves further, nanowires arrays can form segment by segment and thus become longer and longer, when the nanowires become too long ultimately resulting in a WPOP surface (Figure 4 (II) and Figure 2 (a)). However, with the prolong of anodization time, the joint between the top side walls and the bottom of the Al_2O_3 porous layer was etched and becomes thin due to relatively higher acid gradient, which eventually leads to the formation of needle-like nanowires arrays (Figure 4 (III) and Figure 2 (c)). These high-aspect-ratio nanowires will aggregate together from the diverse directions and form a nanowire bunches-like morphology, they will tend to collapse and lean against each other because of the gravity and stirring effects (Figure 4 (IV) and Figure 2 (i)). According to the theory of Park-hutik [13], the formation process of WPOP is a dynamical competition reaction between nanopores formation and nanopores dissolution. We also believe that the following parameters will accelerate the formation of WPOP: ① The room temperature (25℃) and long anodizing time will cause a large amount of heat inside the reaction system, it may lead to serious volume expansion phenomenon of sample, which will accelerate the dissolution of Al_2O_3 nano-walls and make nano-pores crack [14].

Therefore, in order to prevent the nano-pores walls from dissolving too fast to observe the change of the intermediate, it's very important to maintain the temperature of the electrochemical reaction system about 10 ± 0.5 ℃ with ice bags in our experiment. ② as the corrosion of acidic electrolyte accelerates the dissolution of alumina nano-walls, oxalic acid with weak acidity was used, the current density was controlled about 15~20 mA/cm^2. ③ If there are foreign elements in the raw materials, the foreign atoms will not only affect the distribution of electric field dissolution, but also strongly affect the dissolution rate of nano-pores walls [15]. These foreign metal ions or impurities will replace the original lattice point of aluminum, destroy the array of Al atoms, lead to the interruption of lattice period, and eventually lead to the irregular arrangement of nano-pores in the Al_2O_3 film, therefore, 99.99% of the high purity Al was used as the substrate in our experiment [16].

0.1 ml distilled water droplets were dropped onto the horizontal surface of the samples to study the static wettability of different Al_2O_3 films surface. It can be seen that the CA changes from 88.3º to 158.6°, indicating that the wettability changes from hydrophilic to super-hydrophobic under the influence of the surface pattern. The traditional AAO surface with a CA of 88° (Figure 5 a), water droplets can enter the nanochannels of the nanopores and expel air, which completely confirms to Wenzel state. With the increase in the time of the third-step oxidation, the surface of the Al_2O_3 film was continuously etched, the micro-/nano- dual-scale structure of the surface becomes clearer, the WPOP structure shows hydrophilicity due to the increases in roughness continuously (Figure 5 b).

However, the needle-like alumina surface has the strongest hydrophobicity, correspond to the time of third-step oxidation of 50 min (Figure 5 d), in this case, the bubble extrusion phenomenon can hardly be seen between the droplet and the surface, the CA of needle-like Al_2O_3 surface can reach 158.6º, which means a super-hydrophobic state, and indicates that the wetting state changes from Wenzel to Cassie. At the same time, we found that the "hill-like" and "filamentous" WPOP surfaces both showed hydrophobic properties and provided CA of 153.4º and 151.2º (Figure 5 c and e), and

the surface roughness was reduced relative to the needle-like structure. Since the depth of our samples are greater than 1.7 lm, it is an exclusion factor affecting wettability, and the surface morphology with micro/nano dual-scale structure is considered to be the main reason to obtain hydrophobicity [17]. Figure 5 (f) shows the formation process of the micro-/nano- dual-scale super hydrophobic Al_2O_3 surface.

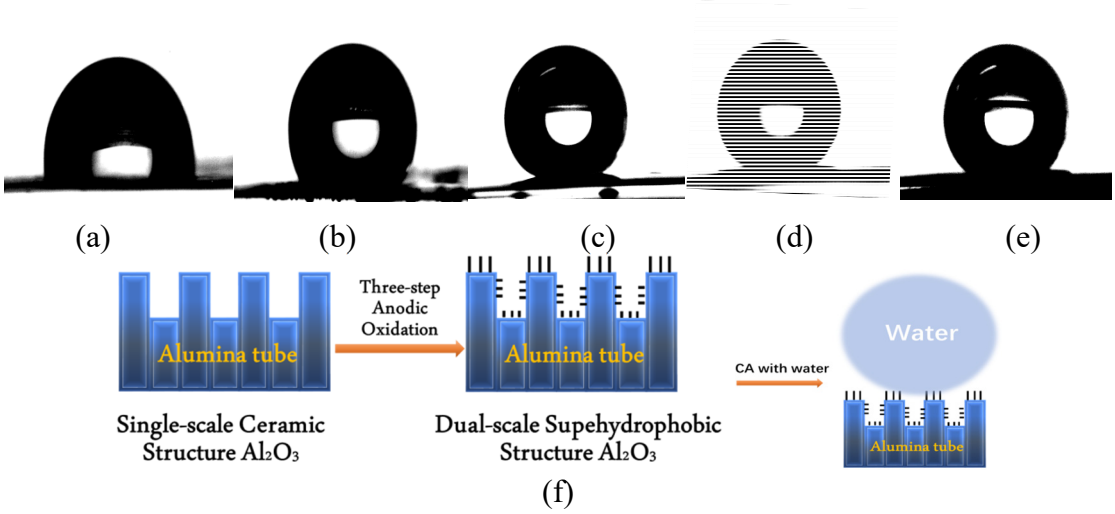

Figure 5. Static photos of CA changes with distilled water as the oxidation time of Al_2O_3 increases. The gradient of 0.05 ml water droplets on the Al_2O_3 horizontal interface changes along the X direction. As the oxidation time increases, the CA of water is 88.3°, 133.6°, 153.4°, 158.6° and 151.2° respectively. Dropping speed is 0.05 ml/s.

4. Conclusion

In this paper, three kinds of Al_2O_3 film with lotus leaf like super-hydrophobic surface were prepared by controlling the third-step anodization time directly. The co-action of lateral distribution of electric field and oxalic acid auxiliary in the inner layer of the AAO film resulting in the dissolution of pore walls, at long last, the needle-like nanostructure accumulated into clusters left on the porous surface and formed micro/nano dual-scale super-hydrophobic structure surface.

References

[1] J. van der Geer, J.A.J. Hanraads, R.A. Lupton, The art of writing a scientific article, J. Sci. Commun. 163 (2000) 51-59. Aslam R, Mobin M, Aslam J, et al. Sugar Based N, N'-didodecyl-N, N' Digluconamideethylenediamine Gemini Surfactant as Corrosion Inhibitor for Mild Steel in 3.5% NaCl Solution-effect of Synergistic KI Additive, J. Scientific Reports, 2018, 8(1): 3690.

[2] Kim D H, Kim Y, Kang J W. Inclined-wall Regular Micro-pillar-arrayed Surfaces Covered Entirely with An Alumina Nanowire Forest and Their Improved Superhydrophobicity, J. Journal of Micromechanics and Microengineering, 2011, 21(7): 075024.

[3] Tettey K E, Dafinone M I, Lee D. Progress in Superhydrophilic Surface Development, J. Materials Express, 2011 1(2): 89-104.

[4] Colin R Crick, Ivan P Parkin. Water Droplet Bouncing-a Definition for Superhydrophobic Surfaces, J. Chemical Communications, 2011, 47(44): 12059-12061.

[5] Cao L, McCarthy T J. “Lotus Effect” Explained? Two Reasons Why Two Length Scales of Topography Are Important, J. Langmuir, 2006, 22(7): 2966-2967.

[6] Cortese B, Amone S D, Manca M, et al. Superhydrophobicity Due to the Hierarchical Scale Roughness of PDMS Surfaces, J. Langmuir the Acs Journal of Surfaces & Colloids, 2008, 24(6): 2712-2718.

[7] Norek M, Putkonen M, Zaleszczyk W, et al. Morphological, Structural and Optical Characterization of SnO2, Nanotube Arrays Fabricated Using Anodic Alumina (AAO) Template-assisted Atomic Layer Deposition, J. Materials Characterization, 2018, 136: 52-59.

[8] Zhao W Y, Zhu R J, Jiang J Y, et al. Environmentally-friendly Superhydrophobic Surface Based on Al2O3@KH560@SiO2 Electrokinetic Nanoparticle for Long-term Anti-corrosion in Sea Water, J. Applied Surface Science, 2019, 484: 307-316.

[9] Wojciechowski J, Szubert K, Peipmann R, et al. Anti-corrosive Properties of Silane Coatings Deposited on Anodised Aluminium, J. Electrochimica Acta, 2016, 220: 1-10.

[10] Bandeira R M, Van Drunen J, Garcia A C, et al. Influence of The Thickness and Roughness of Polyaniline Coatings on Corrosion Protection of AA7075 Aluminum Alloy, J. Electrochimica Acta, 2017, 240: 215-224.

[11] Roach P, Shirtclife N J, Newton M I. Progess in Superhydrophobic Surface Development. Soft Matter, 2008, 4(2): 224-240.

[12] Wu B H, Zhu L W, Ou Y, et al. Systematic Investigation on the Formation of Honeycomb-Patterned Porous Films from Amphiphilic Block Copolymers. The Journal of Physical Chemistry C, 2015,119.4: 1971.

[13] Kotobuki M, Suzuki Y, Munakata H, et al. Effect of Sol Composition on Solid Electrode/Solid Electrolyte Interface for All-solid-state Lithium Ion Battery, J. Electrochimica Acta, 2011, 56(3): 1023-1029.

[14] Ibarra-Castanedo C, Piau J M, Guilbert, et al. Comparative Study of Active Thermography Techniques for the Nondestructive Evaluation of Honeycomb Structures, J. Research in Nondestructive Evaluation, 2009, 20(1): 1-31.

[15] Gerengi H, Mielniczek M, Gece G, et al. Experimental and Quantum Chemical Evaluation of 8-Hydroxyquinoline as a Corrosion Inhibitor for Copper in 0.1 M HCl, J. Industrial & Engineering Chemistry Research, 2016, 55(36): 9614-9624.

[16] Oguzie E E, Li Y, Wang F H, et al. Effect of 2-amino-3-mercaptopropanoic Acid (cysteine) on The Corrosion Behaviour of Low Carbon Steel in Sulphuric Acid, J. Electrochim Acta, 2007, 53: 909-914.

[17] C. D. Smith and E. F. Jones, “Load-cycling in cubic press,” in Shock Compression of Condensed Matter-2001, AIP Conference Proceedings 620, edited by M. D. Furnish et al. American Institute of Physics, Melville, NY, 2002, pp. 651–654.